Theor Chem Account (2008) 121:201–207
DOI 10.1007/s00214-008-0466-z

REGULAR ARTICLE

DFT and ab initio study on the reaction mechanism of $CH_2SH + O_2$

Yi-Zhen Tang · Ya-Ru Pan · Jing-Yu Sun · Hao Sun · Rong-Shun Wang

Received: 22 May 2008 / Accepted: 9 July 2008 / Published online: 5 August 2008
© Springer-Verlag 2008

Abstract The mechanism for the $CH_2SH + O_2$ reaction was investigated by DFT and ab initio chemistry methods. The geometries of all possible stationary points were optimized at the B3LYP/6-311+G(d,p) level, and the single point energy was calculated at the CCSD(T)/cc-pVXZ(X = D and T), G3MP2 and BMC-CCSD levels. The results indicate that the oxidation of CH_2SH by O_2 to form $HSCH_2OO$ is a barrierless process. The most favorable channel is the rearrangement of the initial adduct $HSCH_2OO$ (IM1) to form another intermediate $H_2C(S)OOH$ (IM3) via a five-center transition state, and then the C–O bond fission in IM3 leads to a complex $CH_2S\cdots HO_2$ (MC1), which finally gives out to the major product $CH_2S + HO_2$. Due to high barriers, other products including *cis*- and *trans*-HC(O)SH + HO could be negligible. The direct abstraction channel was also determined to yield $CH_2S + HO_2$, with the barrier height of 22.3, 18.1 and 15.0 kcal/mol at G3MP2, CCSD(T)/cc-pVTZ and BMC-CCSD levels, respectively, it is not competitive with the addition channel, in which all stationary points are lower than reactant energetically. The other channels to produce *cis*- and *trans*-CHSH + HO_2 are also of no importance.

Keywords $CH_2SH \cdot O_2 \cdot$ Transition state · Mechanism

Electronic supplementary material The online version of this article (doi:10.1007/s00214-008-0466-z) contains supplementary material, which is available to authorized users.

Y.-Z. Tang · Y.-R. Pan · J.-Y. Sun · H. Sun · R.-S. Wang (✉)
Institute of Functional Material Chemistry,
Faculty of Chemistry, Northeast Normal University,
Renmin Road 5268, Changchun, Jilin 130024,
People's Republic of China
e-mail: wangrs@nenu.edu.cn

Y.-Z. Tang
e-mail: tangyz171@nenu.edu.cn

1 Instruction

The combustion of the organic sulphur compounds and coals rich in sulphur can produce methylthiyl radical, CH_3S and its isomer CH_2SH, which are important intermediates [1–3] and toxic atmospheric contaminants. It is firmly believed to be one of the key intermediates of OH-initiated oxidation of DMS, especially in areas where the amounts of NO_3 and IO are low enough not to compete with the OH oxidation. For the nonce, the researches focus on two aspects of CH_3S and CH_2SH, (1) the characters of special species, such as spectrum and thermochemistry; (2) the kinetics and mechanisms of reactions involving CH_2SH and CH_3S.

The reactions of CH_3S with some species, such as O_2, O_3, NO_2, and NO have been investigated widely [4–9]. Moreover, it was testified by experiments that the main way to take off CH_3S from atmosphere is its reactions with O_3 and NO_2, respectively. However, little attention has been paid to the reactions of CH_2SH. In 1992, Anastasi et al. reported the rate constant of 8.5×10^{-12} cm^3 molecule^{-1} s^{-1} at 1 atm and 298 K for the reaction of $CH_2SH + O_2$ with the pulse radiolysis/kinetic absorption technique employed [10]. Two possible reaction routes were presumed:

$$CH_2SH + O_2 \rightarrow HSCH_2OO \quad (1)$$

$$CH_2SH + O_2 \rightarrow CH_2SH + HO_2 \quad (2)$$

They proposed that the title reaction proceeds via addition. Although the mechanisms of $CH_2OH + O_2$, similar to the title reaction have been studied extensively [11–14], no result was reported for the mechanisms of this reaction. In this paper, we studied the title reaction with high-level quantum methods for the first time, hoping it is beneficial to further experimental and theoretical studies.

2 Computational methods

Only the doublet potential energy surface (PES) on the lowest electronic states is investigated in this work. Density Functional Theoretical and ab initio calculations are carried out using the Gaussian 03 programs [15]. The geometries of reactants (R), transition states (TS), intermediates (IM), molecular complexes (MC), and products (P) are optimized employing the B3LYP method with the 6-311+G(d,p) basis set. B3LYP method was proved to be an economic and accurate computational model for predicting electronic structure, and has been employed widely. Compared with other levels of theory, the B3LYP method was found to be sufficiently accurate for predicting reliable geometries of the stationary points, at the same time, it is not expensive computationally for scanning the potential energy surface. To determine the nature of all species and the zero-point energy (ZPE) corrections, harmonic vibrational frequencies were calculated at the same level. The number of imaginary frequency (0 or 1) confirms whether it is a local minimum or a transition state. Subsequently, the intrinsic reaction coordinate (IRC) paths were calculated at the same level to verify the transition states connect to the right reactants and products. To check the influence of basis set, the 6-311+G(3df,3pd) basis set is also employed with B3LYP method to optimize the geometries of some intermediates and transition states. In order to obtain more reliable energy on the potential energy surface (PES), the single point energy calculations were performed at the higher levels of G3MP2 [16,17], BMC-CCSD [18,19] and CCSD(T)/cc-pVXZ (X = D and T).

BMC-CCSD scheme was detailed elsewhere, and only a brief description is given here. Single-point-energy evaluations were performed at the CCSD/6-31B(d) and MP2/MG3 levels of theory, respectively. Finally, the energy expression for BMC-QCISD is given in:

$$
\begin{aligned}
&E(\text{BMC-CCSD}) = E(\text{HF/6-31 B(d)}) + c_{\text{H}}(\text{HF/MG3}|\\
&\quad \text{6-31 B(d)}) + c_1\Delta(\text{MP2}|\text{HF/6-31 B(d)})\\
&\quad + c_2\Delta(\text{MP2}|\text{HF/MP2}|\text{6-31 B(d)})\\
&\quad + c_3\Delta(\text{MP4(DQ)}|\text{MP2/6-31 B(d)})\\
&\quad + c_4\Delta(\text{CCSD}|\text{MP4(DQ)/6-31 B(d)}) + E_{\text{SO}}
\end{aligned}
$$

where

$$
\Delta E(\text{L2}|\text{L1/B}) = E(\text{L2/B}) - E(\text{L1/B}) \quad \text{and}
$$

$$
\Delta E(\text{L/B2}|\text{B1}) = E(\text{L/B2}) - E(\text{L/B1}).
$$

And $c_{\text{H}}, c_1, c_2, c_2, c_3$, and c_4 take values of 1.06047423, 1.09791, 1.33574, 0.90363, and 1.55622, respectively.

3 Results and discussion

The geometries of all reactants, products, possible intermediates (IM), molecular complexes (MC) and transition states (TS) involved in the reaction of CH_2SH with O_2 are shown in Fig. 1 (the Cartesian coordinates of all stationary points involved in the CH_2SH reaction with O_2 are provided in supplementary material, Table 1S). The PES of the title reaction at the BMC-CCSD level is depicted in Fig. 2. Table 1 exhibits the ZPE corrections, relative energies (ΔE, relative to the reactants of $CH_2SH + O_2$), reaction enthalpies (ΔH), reaction Gibbs free energies (ΔG) and T1 diagnostic values at the B3LYP/6-311+G(d,p), CCSD(T)/cc-pVXZ (X = D and T), BMC-CCSD and G3MP2 levels. From Table 1 we can see that the energy obtained at the higher levels of CCSD(T)/cc-pVDZ and G3MP2 are close to each other, while the values obtained from CCSD(T)/cc-pVTZ level are generally between that from BMC-CCSD and G3MP2 calculations. The energy obtained at the BMC-CCSD level is used in discussion, unless otherwise state.

It is noted that the spin contamination might be significant for such reaction involving a doublet with triplet electronic state to from a doublet electronic state. The UMP2 is often the most sensitive to spin contamination, and it is less common to find any significant spin contamination in DFT calculations. The checks of S2 values in the optimization calculations suggest it is spin contamination could be negligible after annihilation. To assess the multiconfigurational characteristics of the reaction paths, the T_1 diagnostic values of the CCSD(T) wavefunctions are monitored (see Table 1). Evidently, the T_1 diagnostic values of all the species are less than 0.044 expect for TS7, implying a negligible multireference character of the wavefunctions. The large T1 value indicates that the energy of TS7 may not be reliable, fortunately, TS7 is less important to the title reaction.

3.1 Initial reaction of CH_2SH radical with molecular oxygen

The addition of O_2 to the radical center of CH_2SH, C atom, proceeds on a barrierless surface. The newly formed C–O bond in $HSCH_2OO$ intermediate is about 1.46 Å. As shown in Fig. 2 and Table 1, the additional step releases heat of about 26 and 25.3 kcal/mol at BMC-CCSD and CCSD(T)/cc-pVTZ levels. Therefore, the $HSCH_2OO$ radical could be activated. As shown in Fig. 1, the $HSCH_2OO$ intermediate has two isomers in term of different OOCS dihedral angle, i.e., IM1 (79.0°) and IM2 (−80.0°). Both structures in IM1 and IM2 have almost identical parameters except the OOCS dihedral angle. The energy of IM1 is about 0.7 kcal/mol lower than IM2. It is easy for IM1 and IM2 to interconverse to each other with the O–O bond rotating around C–O bond

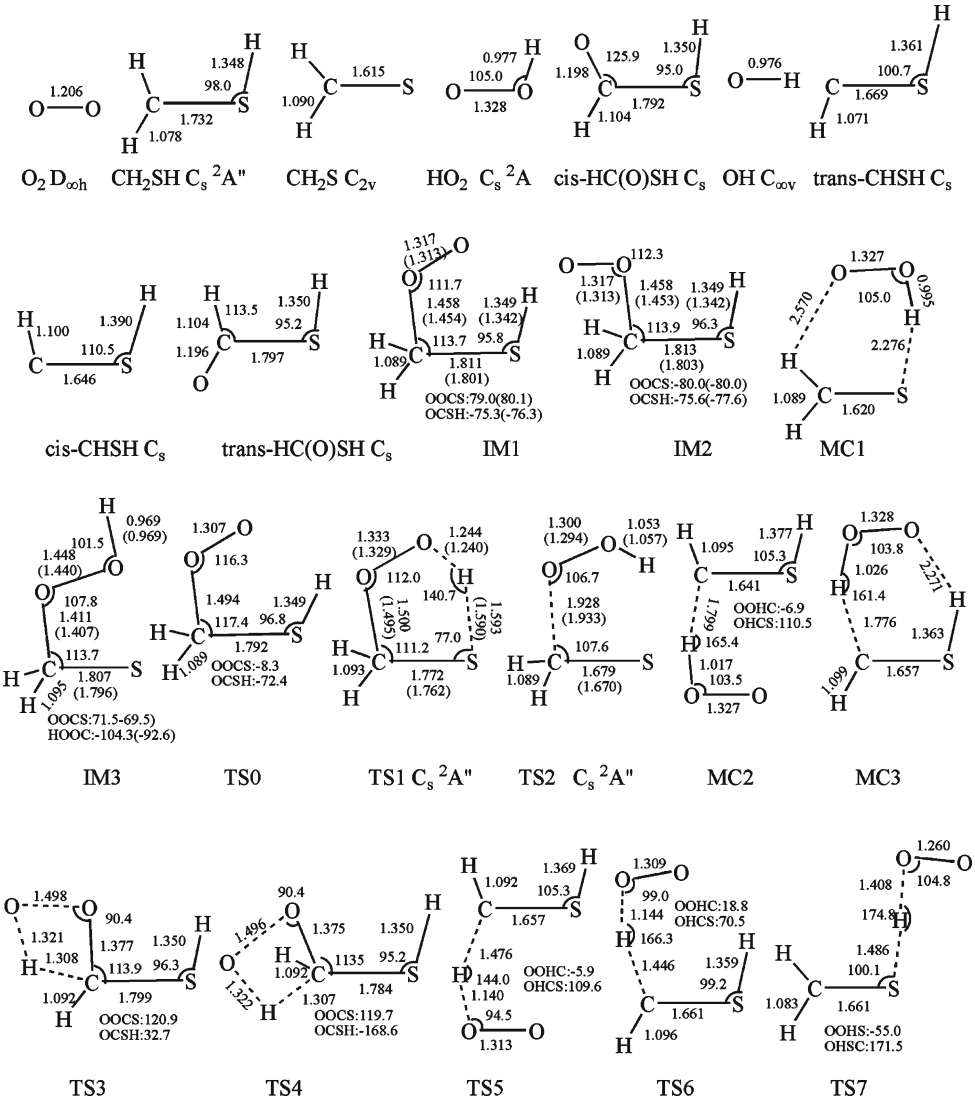

Fig. 1 The optimized geometries of all species for the $CH_2SH + O_2$ reaction at the B3LYP/6-311+G(d,p) level. Bond lengths are in angstroms and angles in degree. In IM1, IM2, IM3, TS1 and TS2, the values in *parentheses* obtained at B3LYP/6-311+G(3df,3pd) level

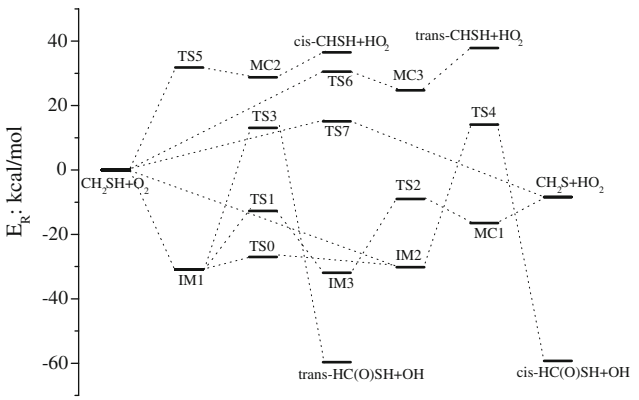

Fig. 2 The profile of PES for the $CH_2SH + O_2$ reaction at the BMC-CCSD//B3LYP/6-311+G(d,p) level

via TS0, in which the OOCS dihedral angle is about −8.0°. TS0 is about −22.5 kcal/mol lower than reactant on the PES. The barrier is 3.5 kcal/mol for the conversion from IM1 to IM2, and the overall $\Delta G^{\neq}$ (298 K) of TS0 is −7.0 kcal/mol. Therefore, it could be predicted that the oxidation of CH_2SH by O_2 and the conversion of IM1 and IM2 is quite feasible under atmospheric conditions. In addition, the dihedral angle OOCS was scanned in an interval of 10°, and the result is summarized in Fig. 3. Obviously, there are two local minimums and a saddle point along the internal rotation with the dihedral angle OOCS of −80, 80 and −10°, respectively.

With large amounts of available energy deposited into IM1 and IM2, it is feasible for the subsequent isomerization or disassociations to occur.

3.2 Isomerization channel

The $HSCH_2OO$ radical IM1 can isomerise to another intermediate IM3 (SCH_2OOH) via a five-number-ring H-shift transition state TS1 with the H atom transferring from S to the

Table 1 The ZPE, ΔH, ΔG and relative energies ΔE (including ZPE corrections) (in kcal/mol) at B3LYP, CCSD(T)/cc-pVDZ, CCSD(T)/cc-pVTZ, G3MP2 and BMC-CCSD levels, and T1 diagnostic values for important stationary points for the reaction of $CH_2SH + O_2$

Species	ZPE	ΔH	ΔG	$\Delta E1$[a]	$\Delta E2$[b]	$\Delta E3$[c]	$\Delta E4$[d]	$\Delta E5$[e]	T1[f]
$H_2CSH + O_2$	21.9	0.0	0.0	0.0	0.0	0.0	0.0	0.0	
$CH_2S + HO_2$	24.3	−4.1	−2.9	−3.6	−2.9	−5.2	−4.0	−6.0	
cis-HC(O)SH + OH	22.7	−56.5	−54.0	−56.1	−55.0		−56.7	−58.9	
trans-HC(O)SH + OH	22.7	−55.3	−52.9	−55.0	−53.3		−56.2	−58.5	
cis-HCSH + HO_2	21.9	43.0	43.7	43.4	44.4		41.2	37.9	
trans-HCSH + HO_2	22.4	41.5	42.2	42.0	43.2		40.2	37.0	
IM1	26.8	−22.9	−10.9	−21.3	−19.8	−23.7	−21.9	−26.0	0.0258
IM2	26.8	−22.4	−10.3	−20.8	−19.1	−23.0	−21.3	−25.3	0.0255
IM3	28.2	−22.4	−10.1	−20.8	−19.8	−24.9	−22.7	−25.6	0.0135
MC1	25.9	−9.6	−0.1	−8.9	−9.3	−11.3	−9.9	−12.5	
MC2	23.8	31.1	40.1	31.8	35.0		32.2	28.8	
MC3	24.4	27.1	37.7	28.1	29.7		28.1	24.7	
TS0	26.4	−20.0	−7.0	−18.1	−15.8		−18.5	−22.5	
TS1	24.6	−10.4	2.9	−8.4	−2.4	−7.8	−4.5	−10.0	0.0359
TS2	25.8	−5.1	7.7	−3.2	0.5	−3.4	−1.4	−5.1	0.0327
TS3	23.0	17.3	29.8	19.0	21.8		20.2	14.2	
TS4	22.9	18.6	31.1	20.3	23.4		21.3	15.1	
TS5	21.9	30.2	41.1	31.5	37.6		35.1	31.8	
TS6	21.5	27.7	37.5	28.8	36.1		32.7	30.1	
TS7	21.8	6.7	16.7	7.7	21.3	18.1	22.3	15.0	0.0635

[a] $\Delta E1$ is obtained from B3LYP/6-311+G(d,p) level
[b] $\Delta E2$ is obtained from CCSD(T)/cc-pVDZ//B3LYP/6-311+G(d,p) level
[c] $\Delta E3$ is obtained from CCSD(T)/cc-pVTZ//B3LYP/6-311+G(d,p) level
[d] $\Delta E4$ is obtained from G3MP2//B3LYP/6-311+G(d,p) level
[e] $\Delta E5$ is obtained from BMC-CCSD//B3LYP/6-311+G(d,p) level
[f] T1 diagnostic values are obtained from CCSD(T)/cc-pVTZ level

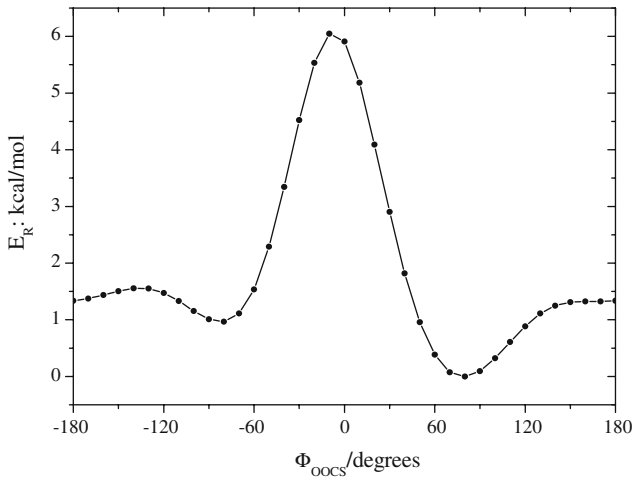

Fig. 3 Energy profile for the internal rotation of $HSCH_2OO$ around $HSCH_2$–O_2 bond. The relative energy (E_R in kcal/mol) was calculated at the B3LYP/6-311+G(d,p) level without ZPE correction

terminal O atom. As shown in Fig. 1, the breaking H–S bond is elongated to be about 1.59 Å, and the forming H–O bond is 1.24 Å. The other geometrical parameters have little change in isomerization. TS1 has C*s* symmetry with a ^{2}A" electronic state. The barrier height is 16 kcal/mol, and TS1 stands at −10 kcal/mol on the PES. In IM3, the O–O bond is stretched to be 1.49 Å, which is about 0.17 Å longer than that in IM1. It is worth noting that the dihedral angles of OOCS and HOOC are about −104 and 72°, respectively. Energetically, IM3 is −25.6 kcal/mol, closing to the energy of IM1 and IM2 on the PES. Subsequently, IM3 could undergo C–O bond fission via TS2. The rupturing C–O bond is stretched to be 1.93 Å, at the same time; the C–S bond is shortened to be 1.68 Å. The IRC calculations at the B3LYP/6-311+G(d,p) level confirm that TS2 goes backward to IM3, and goes forward to give a hydrogen-bond complex $H_2CS\cdots HO_2$, donated as MC1 in Fig. 1. Both TS2 and MC have C_s symmetry with ^{2}A" electronic state. In MC1, the long weak-interaction distance between O and H atom is 2.57 Å, and the S···H hydrogen bond is 2.28 Å. The other geometrical parameters are close to that in product $H_2CS + HO_2$. The barrier height TS2 is 20.6 kcal/mol, however, TS2 lies −5 kcal/mol below the energy of reactant. MC1 finally gives to products $H_2CS + HO_2$. Energetically, MC1 and $H_2CS + HO_2$ are −12.5 and −6 kcal/mol,

respectively. The reaction enthalpy ΔH of this channel is −4.1 kcal/mol at B3LYP/6-311+G(d,p) level, and the overall ΔG is −2.9 kcal/mol. Therefore, this reaction route is feasible to take occur. $H_2CS + HO_2$ is also could be formed by the direct hydrogen abstraction mechanism discussed in the following part. The experimental formation enthalpies of the involved species at 0 K could are available. Due to the lack of experimental formation enthalpy of CH_2SH at 298 K, it is impossible to compare the reaction enthalpy of our result and experimental ones.

From Table 1, it can seen that the energy obtained at CCSD(T)/cc-pVTZ and BMC-CCSD levels is lower than that from G3MP2 and CCSD(T)/cc-pVDZ levels. The result shows that TS1 and TS2 are lower than the initial reactant; therefore, it is evident that the above channel is favorable energetically.

In order to check the influence of basis set, the 6-311+G(3df,3pd) basis set is employed with the same method to reoptimize the geometries of intermediates and transition states involved. The 6-311+G(3df,3pd) basis set, which is useful for describing the interactions between electrons in electron correlation methods, puts 3d functions and 1f function on heavy atoms, and 3p functions and 1d function on hydrogen, as well as diffuse functions on both. The results are summarized in Fig. 1, from which it could be seen, the geometrical parameters are in reasonable agreement with those at the 6-311+G(d,p) level. Most changes in bond length and angles are less than 0.1 Å and 2°, except for the dihedral angle HOOC, in which the difference is about 12°. Therefore, it could be concluded that addition of multiple polarization functions has no significant effect on the title reaction.

3.3 Four-center decomposition of $HSCH_2OO$ radical

The transition states of concerted OH eliminations from $HSCH_2OO$ radical are located at the current level. The corresponding transition state is TS3, which is connected by IM1 and *trans*-HC(O)SH + OH. Another transition state TS4 is found to being connected with IM2 and *cis*-HC(O)SH + OH. The geometrical parameters in TS3 and TS4 are close to each other except the dihedral angle OCSH, which is 33 and −169°, respectively. In both transition states, the breaking of C–H and O–O bond is about 1.31 and 1.50 Å, respectively. Simultaneously, the new forming O–H bond is 1.32 Å, and the C–O bond is shortened by 0.08 Å compared with its equilibrium value in reactant IM1 and IM2. The energy of *trans*-HC(O)SH + OH and *cis*-HC(O)SH + OH are −58.9 and −58.5 kcal/mol, and they are the most stable products on the PES. The barrier heights of TS3 and TS4 are around 40.0 kcal/mol, respectively, even they are 14.2 and 15.1 kcal/mol above reactant. This large energy could be attributed mainly to the expected large strained energy of four-numbered-ring structures. The total $\Delta G^{\neq}$ (298 K) are 29.9 and 31.1 kcal/mol for TS3 and TS4, respectively. Evidently, at room temperature, the two pathways are less favourable compared with isomerization channel.

3.4 Direct hydrogen abstraction mechanism

Transition states of the direct hydrogen abstraction were also found leading to different products. One of the H atoms in CH_2 group abstracted by O_2 will generate HO_2 + *cis*- and *trans*-CHSH via TS5 and TS6, which are product-like transition states, respectively. In TS5 and TS6, the breaking C–H bond is elongated to be 1.45 Å, and the forming O–H bond is about 1.14 Å. The CHO angle is 144° in TS5, and 166° in TS6, which is not linear, and the dihedral angle of OHSH is around 110 and 71°, respectively. Other geometrical parameters stand as spectator. The IRC calculations imply that hydrogen-bond molecular complexes MC2 (*cis*-$CHSH\cdots HO_2$) and MC3 (*trans*-$CHSH\cdots HO_2$) were connected by TS5 and TS6, respectively. It can be seen from Fig. 1, the long distance between H and C atom is about 1.8 Å in MC2, while a six-numbered-ring structure is involved in MC3 with the H···C and O···H bond is about 1.8 and 2.3 Å, respectively. MC2 is about 28.8 kcal/mol on the PES, while MC3 is about 4 kcal/mol lower than MC2. As shown in Fig. 2, both TS5 and TS6 process high barriers, which are 31.8 and 30.1 kcal/mol. The product of HO_2 + *cis*-CHSH and HO_2 + *trans*-CHSH are about 37.0 and 37.9 kcal/mol above reactant. Obviously, with so high barriers and unstable product, the two reaction paths can be negligible, even at combustion condition.

Another channel is hydrogen abstraction by O_2 from SH group leading to $CH_2S + OH_2$. The corresponding transition state is TS7 as shown in Fig. 1. The breaking S–H bond is stretched by 0.14 Å compared with its equilibrium value in CH_2SH, and forming O–H bond is about 1.41 Å. The OHS angle is 175°, which approaches to linear, and the dihedral angle of OOHS is −55°, far away from planar. TS7 is also product-like transition state. The barrier height of TS7 is 15 kcal/mol. With so high barrier, the direct hydrogen abstraction channel can not compete with the addition mechanism states above. It is worth noting that the S^2 is about 1.8 in G3MP2 calculations, and it is around 1.0 even after annihilation. This implies that the spin contamination is significant. Therefore, we optimised TS7 with MP2 and CASSCF methods, but unfortunately, all calculations were failed due to the problem of convergence.

On the other hand, the S^2 is about 0.78 and 0.76 in CCSD(T)/cc-pVTZ and BMC-CCSD calculations, and it is 0.75 after annihilation. From Table 1, we can see that T1 diagnostic value of TS7 is 0.0635, which is much larger than "benchmark" 0.044. The large T1 value indicates that the energy of TS7 may not be reliable, and the nondynamical electron correlation effect is significant in TS7. Fortunately,

TS7 is less important to the title reaction. The energy of TS7 is about 4.2 and 7.3 kcal/mol lower than the value of 22.3 kcal/mol obtained from G3MP2 calculations. All evidences suggest that the energy from CCSD(T)/cc-pVTZ and BMC-CCSD calculations is more accurate than the one from G3MP2. However, the direct hydrogen abstraction channel to yield $CH_2S + HO_2$ is not competitive with the addition reaction route at atmospheric condition.

In summary, five product and six reaction channels were located for the reaction of CH_2SH with O_2 at the B3LPY/6-311+G(d,p) level. In view of energy, with all stationary points involved below reactant, the most favourable channel is the addition of O_2 and CH_2SH to form $HSCH_2OO$ radical IM1, which rearranges subsequently to another intermediate IM3 via a five-numbered-ring transition state, and finally gives out to $CH_2S + HO_2$ via a simple C–O bond fission. With high barrier involved, the direct hydrogen abstraction channel to yield $CH_2S + HO_2$ cannot compete with the addition channel. Other channels forming HC(O)SH + OH and CHSH + HO_2 could be negligible. It is in accordance with Anastasi's [10] experiment that absorption spectra suggested the title proceeds via addition rather than direct abstraction.

3.5 Comparisons with $CH_2OH + O_2$ and $CH_3S + O_2$ reactions

It is very useful to compare the PES feature of the $CH_2SH + O_2$ reaction with that of the analogous one $CH_2OH + O_2$, which have been investigated extensively by experimental and theoretical chemists [11–14]. The main product is $CH_2O + HO_2$, and the reaction processes by a concerted HO_2 elimination from the initial adduct.

First, the comparisons of theoretical results indicate that both reactions undergo a barrierless addition way, i.e., $CH_2XH + O_2 \rightarrow HXCH_2OO$ (X = O and S). It is in accordance with Olivella, Dibble and Schocker. Contrast to Nebot-Gil's [13] report that a transition state of the entrance channel was located at UMP2/6-31G(d) and QCISD/6-31G(d) levels, in which the forming C–O bond is more than 2.1 Å, and the spin contamination was very large. Second, although the addition step is similar, the mechanism is different. The calculations for $CH_2OH + O_2$ could take occur by a concerted step via a five-numbered-ring structure transition state to give out a complex. A four-numbered-ring transition state was also determined by Olivella et al. [12] in concerted step at the CASSCF/6-311G(d,p) level. Although many attempts was made, the transition states involving in concerted HO_2 elimination were not located at various methods and basis sets due to problem of convergence in the optimization for the title reaction. Third, only stepwise HO_2 elimination was found at the B3LYP/6-311+G(d,p) level, which was also determined in $CH_2OH + O_2$ reaction by Schocker [14] and Olivella [12]. It is worth noting that in Olivella's investigation, only two transition states were found at UB3LYP/6-311G(d,p) level, namely, five-numbered-ring transition state in concerted HO_2 elimination and a transition state involving C–O bond fission in $CH_2(O)OOH$ radical. In our calculations, a five-center transition state (TS1) is also located, however, TS1 connect to $CH_2(S)OOH$ (IM3) rather than IM1. Both reactions involve a molecular complex with HO_2 and CH_2X (X = O and S) locating in the same plane, as reported by Olivella and Schocker.

The last difference between $CH_2OH + O_2$ and $CH_2SH + O_2$ reactions is the direct hydrogen abstraction mechanism was not found in the former. All theoretical results reveal that direct abstraction transition state was not located. In the title reaction, the direct abstraction was determined. The spin contamination is not significant in B3LYP optimization; however, it is significant in G3MP2 calculations. Therefore, it is guessed that this transition state has multireference character. Unfortunately, the geometry reoptimised with CASSCF method was failed. The similarities and differences imply that different atoms in the same family of the periodic table have different chemistry.

On the other hand, the reaction of $CH_3S + O_2$, also important in combustion chemistry, attracts many attentions of atmospheric chemists [20,21]. It is also important to compare the mechanisms of $CH_3S + O_2$ with $CH_2SH + O_2$ reactions. The main product in the $CH_3S + O_2$ reaction is $CH_3 + SO_2$ reported by Zhang [20] and Bozzelli [21]. It could be found that both the addition of O_2 to CH_2SH and CH_3S process a barrier-free addition step, but the reaction center is C atom in CH_2SH, while S atom in CH_3S. It is easy to understand because of the different site that lone electron is locating. The dominant channel is analogues to that of $CH_2SH + O_2$ reaction, that is, the initial adduct (CH_3SOO) isomerises to another intermediate CH_3SO_2 via a three-numbered-ring transition state. Subsequently, the rupture of C–S bond in CH_3SO_2 radical leads to the final product $CH_3 + SO_2$. The broken C–S bond is 2.4 Å in Bozzelli's investigation [21], indicating that is weak interaction. Alternatively, surmounting another three-center transition state, CH_3SO_2 radical could rearrange to CH_3OSO, and then the C–O is stretched gradually to give out $CH_3 + SO_2$. The C–O bond is around 2.2 Å reported by Zhang and Bozzelli.

The direct abstraction transition state was also found in $CH_3S + O_2$ reaction to form $CH_2S + HO_2$, which is the main product in $CH_2SH + O_2$ reaction. Other products such as $CH_3O + SO$, $CH_2O + SHO$ or HSO and $CH_3SO + O$ could be negligible for the $CH_3S + O_2$ reaction.

4 Conclusions

The reaction mechanisms of the CH_2SH oxidation by molecular oxygen were studied detailedly with ab initio and DFT

methods for the first time. All stationary points involved in the title reaction were optimized at the B3LYP/6-311+G(d,p) level, and more accurate energies were calculated at G3MP2,CCSD(T)/cc-pV*X*Z(*X* = D and T) and BMC-CCSD levels. The results reveal that seven transition states, three intermediates, a molecular complex and five possible products were involved on the ground state potential energy surface. Addition and direct abstraction mechanisms were determined, and the former one is dominant. The most favorable channel involves the association of CH_2SH with O_2 to form $HSCH_2OO$ radical(IM1) via a barrierless process, which could rearrange to another intermediate $CH_2(S)OOH$ (IM3) via a five-center transition state. Subsequently, the C–O bond fission of IM3 leads to a molecular complex, $CH_2S\cdots HO_2$, which gives out to $CH_2S + HO_2$ finally. The other products including *cis* and *trans*-HC(O)SH + OH could be negligible due to high barrier heights. The direct hydrogen abstraction yields either *cis*- and *trans*-CHSH + HO_2 or $CH_2S + HO_2$. However, all of them proceed significant barrier heights; therefore, they are of no importance compared with the addition mechanism. Our results are in good agreement with experimental conclusion.

Acknowledgments This work was supported by the National Natural Science Foundation of China (No. 20773021) and the Science Foundation for Young Teachers of Northeast Normal University (No. 20070315). We are greatly thankful for the referees' helpful comments.

References

1. Atkinson R, Pitts JN Jr, Aschrmann SM (1984) J Phys Chem 88:1584. doi:10.1021/j150652a029
2. Yin F, Grosjean D, Seinfeld JH (1990) J Atmos Chem 11:309. doi:10.1007/BF00053780
3. Wine PH, Kreutter NM, Gump CA, Ravishankara AR (1981) J Phys Chem 85:2660. doi:10.1021/j150618a019
4. Tyndall GS, Ravishankara AR (1989) J Phys Chem 93:2426. doi:10.1021/j100343a041
5. Martinez E, Albaladejo J (2000) Atmos Environ 34:5295. doi:10.1016/S1352-2310(00)00348-4
6. Wang SK, Zhang QZ, Zhou JH, Gu YS (2004) Acta Chimi Sin 62:550
7. Martinez E, Albaladejo J (1999) Chem Phys Lett 308:37. doi:10.1016/S0009-2614(99)00579-5
8. Chang PF, Wang TT, Wang NS (2000) J Phys Chem A 104:5525. doi:10.1021/jp000294a
9. Tang YZ, Sun H, Pan YR, Wang RS (2007) Int J Quantum Chem 107:1495. doi:10.1002/qua.21291
10. Anastasi C, Broomfield M (1992) J Phys Chem 96:696. doi:10.1021/j100181a034
11. Dibble TS (2002) Chem Phys Lett 355:193. doi:10.1016/S0009-2614(02)00211-7
12. Olivella S, Bofill JM, Solé A (2001) Chem Eur J 7:3377. doi:10.1002/1521-3765(20010803)7:15<3377::AID-CHEM3377> 3.0.CO;2-8
13. Ramírez-Ramírez VM, Serrano-Andrés L, Nebot-Gil I (2006) Theor Chem Acc 116:637. doi:10.1007/s00214-006-0109-1
14. Schocker A, Uetake M, Kanno N, Tonokura K (2007) J Phys Chem A 111:6622. doi:10.1021/jp0682513
15. Frisch MJ, Trucks GW, Schlegel HB, Scuseria GE, Robb MA, Cheeseman JR, et al (1998) Gaussian 03; Gaussian, Pittsburgh PA
16. Curtiss LA, Raghavachari K, Redfern PC, Pople JA (1998) J Chem Phys 109:7764. doi:10.1063/1.477422
17. Baboul AG, Curtiss LA, Raghavachari K (1999) J Chem Phys 110:7650. doi:10.1063/1.478676
18. Fast Pl, Corchado JC, Truhlar DG (1999) J Phys Chem A 103: 5129 doi:10.1021/jp9903460
19. Lynch BJ, Zhao Y, Truhlar DG (1999) J Phys Chem A 109:1643. doi:10.1021/jp045847m
20. Zhang HT, Zhou ZY, Jalbout AF (2003) THEOCHEM 663:73. doi:10.1016/j.theochem.2003.08.068
21. Zhu L, Bozzelli JW (2006) J Phys Chem A 110:6923. doi:10.1021/jp056209m